

Statistical Optical Link Budget Analysis

Hua Xie and Kar-Ming Cheung
Jet Propulsion Laboratory
California Institute of Technology
Pasadena, CA 91109-8099

Hua.Xie@jpl.nasa.gov, Kar-Ming.Cheung@jpl.nasa.gov

Abstract—In this paper, we describe work on extending statistical analysis methods to optical communications links, with a primary focus on intensity modulated, direct detected photon-counting channel utilizing pulse-position-modulation (PPM). We performed analysis on the relationship between bit error rate (BER) requirement, statistical characteristics of the received signal power and noise power, and the coded performance curves. We presented link analysis results with preliminary uncertainty quantifications of signal power and noise power. We used the Consultative Committee for Space Data Systems (CCSDS) Serially Concatenated convolutionally coded Pulse Position Modulation (SCPPM) prototype software [1] to obtain coded performance curves under different operating conditions with varying signal power, background noise power, code rates, and PPM modulation orders. Comparison with traditional, deterministic analysis shows that extra margin needs to be reserved to compensate for the performance losses caused by uncertainties of the link parameters.

TABLE OF CONTENTS

1. INTRODUCTION.....	1
2. REVIEW OF COMMUNICATION LINK ANALYSIS....	2
3. FLUCTUATIONS IN THE RECEIVED SIGNAL AND NOISE POWER	3
4. LINK MARGIN IN STATISTICAL OPTICAL LINK ANALYSIS	4
5. MODELING AND SIMULATION	4
6. CONCLUSION AND FUTURE WORK	5
ACKNOWLEDGMENTS	6
REFERENCES	6
BIOGRAPHY	6

1. INTRODUCTION

Communication link analysis is a system engineering tool that is used to evaluate mission data return capability and develop requirements in communication system design. The purpose of link analysis is to determine if a target data rate can be supported with a given communication link condition, and if so, with what margin. Communication link analysis is inherently statistical due to uncertainties associated with different components of the system. Traditional approach in link budgeting assumes deterministic, often conservatively estimated, values for the link parameters to accommodate adverse conditions. This can result in a system design that does not optimize achievable data rates.

J. Yuen formulated the framework of statistical RF link analysis in the 1970s [2]. This framework exploited the additive nature of the RF link equation (gain and loss parameters are expressed in dB domain) and proposed to use Gaussian distribution to approximate the received signal-to-noise ratio

(SNR) term under the assumption that link parameters are independent random variables. One can then design the communication link based on statistical confidence levels measured in terms of the standard deviation of the received SNR. Cheung extended this framework and proved in [3] that the Gaussian approximation is valid under the Lyapunov's condition where no single link parameter has dominant variance over the others.

Cheung demonstrated in [4] that this statistical link analysis approach can provide insights on the design choices of coding scheme and link margin for reliable data delivery over RF links. The author invoked a variant of the Central Limit Theorem that provides the sufficient condition for using Gaussian approximation to model the distribution of the link SNR. It was shown that a weighted sum of Gaussian variables with shifted means can be used when there are one or more dominant components, e.g., weather effects in Ka-band, in the link. Statistically “adjusted” coded performance curves were produced by convolving the ideal coded performance curve with the probabilistic density function of the SNR. This work provides a methodology for system engineers to derive statistical link operating points under different quality of service requirements and weather availability assumptions.

In order to extend this framework to optical link budget analysis, we need to construct an integrated performance modeling approach with a validated set of input distributions. However, unlike a coherent RF link, the capacity of a direct-detected PPM link does not have a closed form representation except in noiseless case. Even though an asymptotic approximation is available [5] to provide us with some insights in understanding the high-level tradeoffs between input parameters and their first-order impacts on link performance, the fundamental deviation of the optical link model from a simple linear equation does not lend us to derive a straightforward extension of the statistical RF link analysis [4]. In this article, we adopted a numerical approach which obtains the statistically “adjusted” performance by convolving the average coded performance curves with probabilistic distributions of the signal and noise power.

Under a deterministic optical link analysis approach, one will derive the design points, i.e., required signal power to meet the BER tolerance, from the set of average coded performance curves that are produced for different background noise levels. Each of these design points assumes deterministic average values for both signal and noise power. In order to accommodate signal and noise power fluctuations that can occur due to adverse effects such as weather and non-ideal operation, one would reserve conservative link margins to add to the required signal power. This often leads to an over-design of the link budget and does not lend itself to optimize the achievable data rates.

In this paper, we show that in absence of noise variation, the effect of signal fluctuations can be characterized as a “fading”

loss in the coded performance. By fading loss we refer to the gap between the two set of curves that represents the additional signal power required for any given BER tolerance. When both signal and noise power fluctuations are present, the link performance degradation worsens towards the high SNR regions. We used the M-ary PPM modulation serially concatenated with a forward error correction (FEC) code (SCPPM) [6] as an exaple in this work. However this framework can be generalized to other types of optical channels. We performed simulations to obtain the coded performance data using the CCSDS SCPPM prototype software [1]. A coded performance “surface” was produced as a collection of coded performance curves at various background noise levels.

Due to lack of access to historical Cumulative Distribution Function (CDF) data of the atmospheric transmittence, optical turbulence, and cloud coverage, we used simulated distribution models that were generated based on the signal and noise characterization in literature [7] [8]. We focused on evaluating the the sensitivity of optical link performance to two of dominating effects, i.e., sky radiance variation and turbulence induced signal power fluctuation.

The rest of this paper is organized as follows. Section 2 provides an overview of optical link analysis approaches. Section 4 describes the role of link margin and the procedure of statistical optical link analysis that takes into account the fluctuations of signal power and noise power. Section 5 shows the deviation of statistical design points from deterministic design points using SCPPM codes [1] as an example. We also compared results for SCPPM with differnt PPM orders $M = \{8, 16\}$ and code rates $R_{FEC} = \{2/3, 1/2\}$. Section 6 concludes this paper and discusses potential future work.

2. REVIEW OF COMMUNICATION LINK ANALYSIS

Link analysis relates the conditions under which a communication link may be used to reliably transmit information. We say a link is closed if the error rate, either at a bit, codeword, or packet level, satisfies a user specified requirement. The threshold on the required signal power depends on the required quality of the received data and error correction coding being used.

In traditional link budget analysis, one would derive the average received signal and noise power [2] [9], look up the required signal power from the capacity or coded performance curve for the target BER, and decide link closure based on the resulting link margin.

RF Link Equation

The capacity of the power constrained RF Gaussian channel is a direct function of the link SNR, as given by [10]:

$$C_{\text{RF}} = W \log_2 \left(1 + \frac{P_r}{kTW} \right) \quad (\text{b/s}) \quad (1)$$

$$\approx \frac{1}{\ln(2)} \frac{P_r}{kT} \quad (\text{b/s}) \quad (2)$$

where W is the bandwidth occupied by the signal, k is Boltzmann’s constant in Joules per kelvin, and T is the system noise temperature in kelvins. Approximation in equation (2) follows from assuming $P_r/kTW \ll 1$, i.e., that one operates in the power, as opposed to bandwidth, limited regime.

RF link analysis then simplifies to an estimation process of the link SNR, which can be performed as an additive equation in the dB domain

$$\frac{P_r}{kT} (\text{in dB}) = EIRP + G - kT (\text{in dB}) - L_{\text{range}} - L_o. \quad (3)$$

$EIRP$ is the effective isotropic radiator power of the transmitter including all the gain and loss terms on the transmission side. The term G includes all the gain and loss terms on the receiver side. L_{range} is the space loss and L_o includes contributions from the intervening transmission media such as atmospheric loss.

Statistical RF link analysis [2] [3] relies on the additive nature of the link equation (3) and characterizes the resulting link SNR statistics using Gaussian approximation, which provides sufficient information for a system engineer to design the link based on statistical confidence levels.

Direct-Detected Optical PPM Link Equation

The capacity of the Poisson PPM channel is a function of the PPM order, and the received noise and signal rates [11]

$$C_{\text{OPT}} = \frac{1}{MT_s} (D(p_1||p_0) - D(p_y||p_{y|0})) \quad (\text{b/s}) \quad (4)$$

where $D(f||g) = E_f \log_2 f/g$ is the relative entropy, p_1 and p_0 are probability mass functions of a signal and noise slot and p_y and $p_{y|0}$ are the probability mass functions of a random PPM symbol and a noise vector, respectively.

Except for noiseless case, evaluating (4) requires one to approximate a multi-dimensional infinite sum or perform a Monte-Carlo simulation. This does not lead to any insight for us to clarify the tradeoffs between the signal power, noise power, and modulation order. An approximate optical PPM link equation was presented in [5] which combines a number of bounds on C_{OPT}

$$C_{\text{OPT}} \approx \frac{1}{\mathcal{E} \ln(2)} \left(\frac{P_r^2}{P_r \frac{1}{\ln(M)} + P_n \frac{2}{M-1} + P_r^2 \frac{MT_s}{\ln(M)\mathcal{E}}} \right) \quad (\text{b/s}) \quad (5)$$

where P_r and P_n are the detected signal and noise power.

As we vary P_r with P_n fixed, we sweep out three regions of operation, depending on which term in the denominator dominates. When $P_r/\ln(M) \gg 2P_n/(M-1)$ and $P_r/\ln(M) \gg P_r^2 MT_s/(\ln(M)\mathcal{E})$, the background noise is negligible, and we are in the (signal) power constrained region. When $2P_n/(M-1) \gg P_r/\ln(M)$ and $2P_n/(M-1) \gg P_r^2 MT_s/(\ln(M)\mathcal{E})$, we are dominated by background noise. At sufficiently large P_r , the third term dominates, the capacity saturates at $\log_2(M)/MT_s$, and we are in the bandwidth constrained region. Depending on the noise power, we may see only two of the three regimes as a function of P_r .

Intuitively we may develop separate analytical forms of the capacity depending on the regimes of the signal and noise power, and adopt the generalized approach in [4]. However due to high sensitivity of an optical link to weather effects, we may be crossing over different regimes during a single pass duration. Furthermore, the Lyapunov’s condition may not hold true for an optical link due to existence of dominating effects such as optical turbulence and pointing-induced fading.

One approach of characterizing the signal statistics is to break down the modeling by separately quantifying the dominating weather-related loss terms and system (i.e., space terminal and ground terminal) related loss terms. The combinational effect of the terminal-related loss terms can be modeled the same way as in a RF link, i.e., Gaussian approximation. Turbulence and pointing induced signal fluctuation effects can be integrated by convolving the distribution functions.

3. FLUCTUATIONS IN THE RECEIVED SIGNAL AND NOISE POWER

During a free space optical communication session, signal can be attenuated by various unpredictable non-ideal operation effects and weather effects. For example, the pointing error causes beam wandering effects which manifest themselves as a dynamic fading of the received signal power; At the receiver there are transmission losses through a narrow band filter, mirror losses, and optical losses, etc. These losses are tied with the specific design/implementation of the terminals and can be measured based on component-level testing of the system.

There have been some existing work that characterized atmospheric attenuation and turbulence effects at some ground stations of interest. For example, extensive simulations were performed to model optical turbulence and cumulative distribution functions (CDFs) were obtained for optical seeing parameter r_0 at various locations of Hawaii [12]; Atmospheric transmittance and cloud-related availability studies were performed at the JPL Table Mountain [13] using historical collection of measured data. Ideally, these collective sets of information can be used to build a weather availability table for statistical optical link analysis, in a simile to the ones used by RF link analysis from DSN 810-005 handbook [14].

Noise enters the receiver via photo-electrons generated from incident background light, dark currents, and thermal noise. In this paper, we assume background noise is dominated by sky radiance. The day time sky radiance dataset, measured by NASA's Aerosol Robotic Network (AERONET), demonstrates a spread of values for any SEP angle. The spread is associated with a range of atmospheric conditions. With standard link analysis approach, one will derive separate design points using the average measured sky radiance values for assumed atmospheric conditions. The fluctuation in received noise power is accommodated typically by incorporating a conservative link margin. This approach can potentially lead to an over-design of the system for any given atmospheric conditions.

Received Signal Power

Without loss of generality, the received signal power in a free space optical link may be factored as

$$P_r = P_t + G_t + G_r - L_s - L_{atm} - L_{pt} - L_t - L_r, \quad (6)$$

where

- P_t is the transmitted power,
- G_t is the transmitter gain,
- G_r is the receiver gain,
- L_s is the range loss,
- L_{atm} is the atmospheric loss,
- L_{pt} is the pointing loss,
- L_t is the transmitter related loss, and
- L_r is the receiver related loss

Space and Ground Terminals—We combined together in L_t all the transmitter related losses, e.g., losses during coupling the laser beam to the optical system, losses in propagation through the optical system, etc. The receiver loss L_r captures all the receiver related losses, such as transmission loss through the narrow band filter, polarization loss, and coupling loss. The distributions of these system specific gain and loss terms can be measured and characterized once the transmitter and receiver design is determined.

Pointing Error and Jitter—In a real operation, the transmitter points to the receiver with a quasi-static pointing error and time varying pointing jitter. The pointing error moves the transmitted beam relative to the receiver, resulting in a dynamic fading of the received signal power. Pointing loss includes a static loss term from pointing error and a faded capacity loss term due to pointing jitter. A link budget was developed that quantified the pointing jitter induced capacity loss in [15], assuming a normal distribution model for the pointing process. A maximum faded capacity loss was accounted to guarantee link closure for a given outage probability. Similar standalone analysis of pointing-induced fading and probability of link outage was presented in [16]. The probability of link outage was derived based on the signal power distributions and capacity of the Poisson PPM channel (4). The average noise power was assumed to be fixed in this development. In this paper we are interested in incorporating pointing-induced signal fading model as one dominant component in our statistical analysis framework.

Atmospheric Loss—As the optical beam is transmitted through the atmosphere, the signal is attenuated due to absorption and scattering. The MODerate resolution atmospheric TRANsmission (MODTRAN) simulation tool [17] can be used to effectively predict attenuation under a range of atmospheric conditions. We are mostly interested in the statistical characteristics of the atmospheric transmittance, which to the best of our knowledge, only exists in empirical forms. For example, JPL's AVM program measured the spectral attenuation through atmosphere using stars as light source for several sites [13]. Cumulative probabilities of atmospheric attenuations were obtained at wavelengths of 1064 nm and 960 nm under various weather conditions.

Power Fluctuation due to Optical Turbulence—Clear air turbulence causes random fluctuations in the received signal intensity [7]. The effects of optical turbulence will manifest themselves in different ways on an uplink beam and a downlink beam. In this paper we focus on the downlink where the turbulence effects can be modeled as a log-normal fading process $v(t)$ [8]

$$f_V(v) = \frac{1}{\sqrt{2\pi\sigma_I^2}} \frac{1}{v} \exp\left(-\frac{(\ln v + \sigma_I^2/2)^2}{2\sigma_I^2}\right), \quad (7)$$

where the variance σ_I^2 is referred to as the scintillation index. Estimates of the scintillation index may be derived from models of the refractive index over the propagation path. Waveoptics simulations were performed in [8] to generate a time series of the signal irradiance for a given atmospheric coherence length $r_0 = 5.2$ cm at Table Mountain. Even though there is no loss in average power, the random variation of received signal irradiance cause a fading loss, which is the increase in required signal power to achieve the specified capacity. An analytic form exists in noiseless case to calculate fading loss and was used in JPL's Deep Space Optical Link budget tool

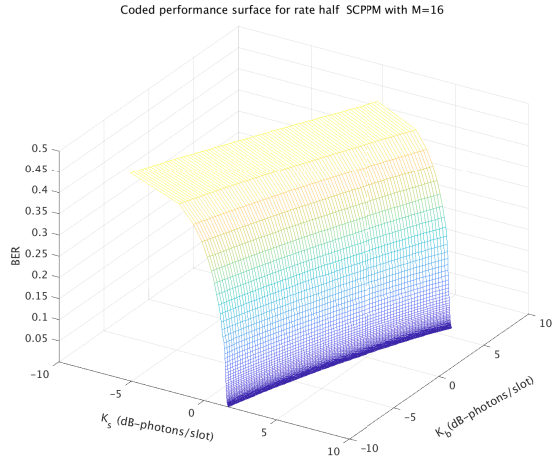


Figure 1. Coded Performance Surface of SCPPM with $R_{FEC} = 1/2$ and $M = 16$.

(DeSOL) [9].

Noise Power

In this paper, we assume background noise is dominated by sky radiance. NASA has a global network of deployed Sun photometers, known as the Aerosol Robotic Network (AERONET), that is used to monitor day time sky radiance. They reported a rich dataset of sky radiance as a function of the position of the Sun in the sky at a few different ground sites. As shown in chapter 3 of [7], the measured sky radiance values demonstrate a spread at any given SEP angle. The spread is associated with a range of atmospheric conditions. Due to lack of access to the empirical CDF of the measured sky radiance, we used simulated sky radiance data generated as Gaussian distributions with statistics obtained from graphs in [7].

4. LINK MARGIN IN STATISTICAL OPTICAL LINK ANALYSIS

In standard optical link analysis, required signal power is derived based on tolerable error rates specified by users. Once the error rate requirement has been specified, the required signal power for each of the design points will be used for telecommunication system design. For a chosen error correction code, e.g., SCPPM with certain code rate and modulation order, the coded performance defines a surface $z = h(x, y)$ over operational range of signal power x and noise power y .

In this paper, we used the CCSDS SCPPM prototype software [1] to obtain coded performance curves under different operating conditions with different average signal power and background noise power. We show in Figure 1 the coded performance surface of SCPPM with $R_{FEC} = 1/2$ and $M = 16$. K_b and K_s are the average noise and signal rates in unit of dB-photons/slot. They relate to the noise and signal power by a constant scaling factor.

Statistically Adjusted Coded Performance

Let's assume x and y are independent and their marginal distributions are denoted by $f(x)$ and $g(y)$, we can obtain

the adjusted coded performance by convolving the original coded performance surface with the input distributions

$$\bar{h}(x, y) = \int_x \int_y h(x, y) f(x) g(y) dx dy. \quad (8)$$

Characterization of the signal power distribution can be broken down to system related effects and weather-related effects. If weather availability models, e.g., cumulative distribution functions of the turbulence and sky radiance, are available, we can integrate the weather availability information using weighted sum of conditional distributions as in [4]. For example, for a given weather availability CD , where $10 \leq CD \leq 99\%$, we define $f(x|\sigma_i)$ to be the conditional distribution of the signal power under the i -th percentile of the turbulence effects. σ_i is the scintillation index of the log-normal signal model produced with the atmospheric coherence length r_o in its i^{th} percentile. The resulting signal power distribution for weather availability CD can be expressed as

$$\bar{f}(x) = \sum_{i=10}^{CD} P_i f(x|\sigma_i). \quad (9)$$

Similarly, we can model the background noise by a weighted sum of Gaussian distributions $\bar{g}(y) = \sum_{i=10}^{CD} P_i g(y|m_i, \sigma_i^n)$, where $g(y|m_i, \sigma_i^n)$ represents the noise distribution under the i^{th} percentile of atmospheric conditions.

5. MODELING AND SIMULATION

We used equation 8 in Section 4 to evaluate the statistically adjusted coded performance for SCPPM with different rates and modulation orders. Below we will use terms signal and noise flux rates, which are scaled versions of signal and noise power, as the input parameters to the performance analysis. We adopted the log-normal signal distribution model as presented in [8] as an example for proof of concept purpose. For background noise, we used simulated Gaussian distribution data with different mean and variances to represent day-time and night-time passes under various weather conditions [7].

Figure 2 shows the coded performance curves, before and after statistical adjustment, of SCPPM with $R_{FEC} = 1/2$ and $M = 16$ at an average background noise flux rate of $K_b = 1$ photons/slot. We assume that the signal flux rate have a log-normal distribution with $\sigma_S = 0.15$ photons/slot. We evaluated the performance degradation for cases where the noise flux is either deterministic or has standard deviation of $\sigma_b = 1.02$ photons/slot.

When fluctuations exist in both signal flux and noise flux, the coded performance curve widens out more in high SNR regions, due to weigh-in of increase in required signal power at the tail of noise flux distributions; When the link uncertainty is dominated by signal flux fluctuation, the coded performance curve simply "shifted" to the right. The gap between the deterministic curve and the shifted curve is often referred as scintillation loss, or atmospheric fading [8].

Figure 3 shows the coded performance curves, before and after statistical adjustment, of Rate 1/2 coded 16-SCPPM, with signal flux rate having a log-normal distribution with

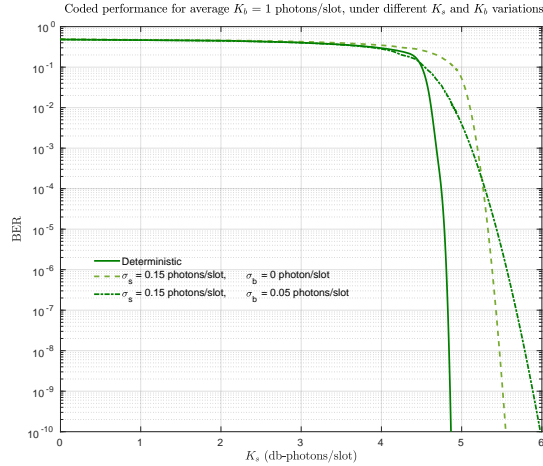


Figure 2. Statistically adjusted BER curves with average noise flux rate of $K_b = 1$ photons/slot. Signal flux rate if log-normal with standard deviation of 0.15 photons/slot.

H

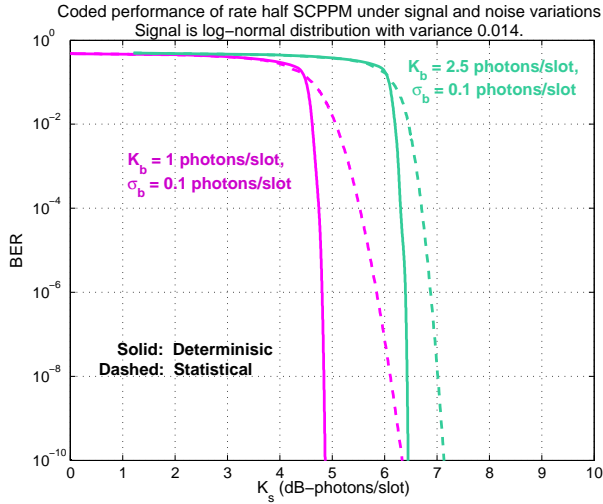


Figure 3. Statistical BER performance under different average noise levels.

$\sigma_s = 0.014$ photons/slot, and average noise flux rates of 1 photon/slot (normal day pass) and 2.5 photons/slot (adverse day pass with small SEP angle). We evaluated the performance degradation for these two scenarios with $\sigma_b = 0.1$ photons/slot for both cases. The two sets of curves demonstrated a transition in the sensitivity of optical link performance to fluctuations in signal and noise power. When the average noise level is low relative to the signal level, link operates in a signal dominant regime. In this case the effects from the tail of the noise distribution affects the performance more profoundly due to transition to noise dominant regime in the tail region. When the average noise flux rate is high and the spread of the noise distribution is small relative to the average noise, the link operates in noise dominant regime consistently. The fluctuation in signal power does not affect the performance as much as in the other case.

Figure 4 compared the coded performances of SCPPM codes

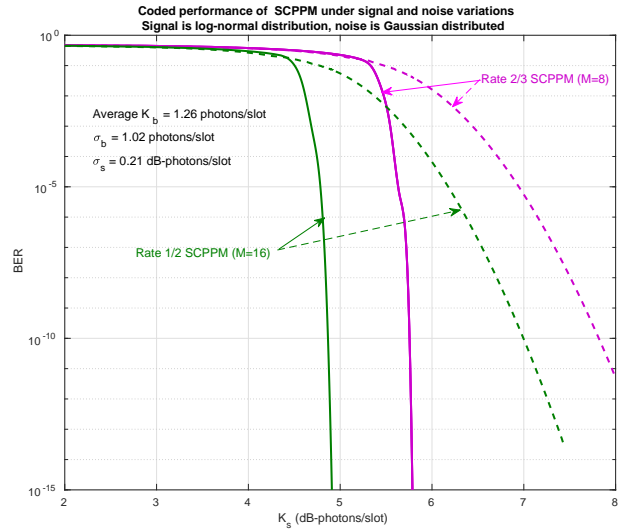


Figure 4. Comparison of statistical BER performance of SCPPM with different code rates and modulation order.

with different rates and modulation orders. The green curves are produced for SCPPM of $R_{FEC} = 1/2$ and $M = 16$. The magenta curves are produced for SCPPM of $R_{FEC} = 2/3$ and $M = 8$. This simulation was performed with average noise flux rate of 1.26 photons/slot (nominal daytime background light) with standard deviation of 1.02 photons/slot. The signal flux rate is log-normal with standard deviation of 1.05 photons/slot. The two configurations of the SCPPM codes demonstrated similar performance degradation.

6. CONCLUSION AND FUTURE WORK

We described a statistical optical link analysis approach that takes into account the inherent uncertainties associated with the link parameters. Optical communications is highly sensitive to atmospheric and weather effects. Using the direct-detected PPM link as an example, we showed the effects of channel turbulence and background noise fluctuation can vary significantly depending on the regime of the design point. For example, when link operates in noise dominant regime, the fading loss caused by turbulence is not as profound as in the signal dominant regime. The shape of the statistically adjusted coded performance curves (i.e. at different average background noise levels) depend on the relative spread of the signal power and noise power with respect to their mean values. When the signal power fluctuation dominates the link uncertainty, the adjusted curve represents a shifted version of the original performance curve, and the degradation can be modeled as a fading loss. On the other hand, when background noise fluctuation dominates, the coded performance curve widens towards high SNR region, caused by weigh-in of the tail distribution of the background noise.

Due to lack of access to historical CDF data of the atmospheric transmittance, optical turbulence, and cloud coverage, we were not able to incorporate weather availability model into our simulation and analysis. We plan to seek and obtain those historical data for several optical ground sites and incorporate the model into our framework.

ACKNOWLEDGMENTS

The research described in this paper was carried out at the Jet Propulsion Laboratory, California Institute of Technology, under a contract with the National Aeronautics and Space Administration. The research was supported by the NASA's Space Communication and Navigation (SCaN) Program.

REFERENCES

- [1] *Optical Communications Coding and Synchronization*. Consultative Committee for Space Data Systems (CCSDS) 142.0-R-1, Red Book, June 2018.
- [2] J. Yuen, Ed., *Deep Space Telecommunication Systems Engineering*. New York: Plenum Press, 1983.
- [3] K.-M. Cheung, "Statistical link analysis - a risk analysis perspective," *The Interplanetary Network Progress Report*, vol. 42-183, November 2010.
- [4] Kar-Ming Cheung, "The role of margin in link design and optimization," in *Aerospace conference, 2015 IEEE*, 2015.
- [5] B. Moision and H. Xie, "An approximate link equation for the direct-detected optical ppm link," *The Interplanetary Network Progress Report*, vol. 42-199, November 2014.
- [6] B. Moision and J. Hamkins, "Coded modulation for the deep-space optical channel: Serially concatenated pulse-position modulation," *The Interplanetary Network Progress Report*, vol. 42-161, May 2005.
- [7] H. Hemmati, *Deep Space Optical Communications*. Wiley, 2006.
- [8] J. H. Bruce Moision, Sabino Piazzolla, "Fading losses on the lcrd free-space optical link due to channel turbulence," vol. 8610, 2013, pp. 8610 - 8610 - 10. [Online]. Available: <https://doi.org/10.1117/12.2010701>
- [9] S. Piazzolla, "Deep space optical link (DeSOL) software," JPL Optical Communications Group, 2008.
- [10] T. M. Cover and J. A. Thomas, *Elements of Information Theory*. Wiley, 1991.
- [11] J. Hamkins, M. Klimesh, R. McEliece, and B. Moision, "Capacity of the generalized ppm channel," in *Information Theory, 2004. ISIT 2004. Proceedings. International Symposium on*, 2004, pp. 334-334.
- [12] R. J. Alliss and B. D. Felton, "Improved climatological characterization of optical turbulence for free-space optical communications," vol. 8162, 2011, pp. 8162 - 8162 - 9. [Online]. Available: <https://doi.org/10.1117/12.898398>
- [13] P. W. Nugent, J. A. Shaw, and S. Piazzolla, "Infrared Cloud Imager Development for Atmospheric Optical Communication Characterization, and Measurements at the JPL Table Mountain Facility," *The Interplanetary Network Progress Report*, vol. 42-192, February 2013.
- [14] "DSN Telecommunications Link Design Handbook," <http://www.deepspace.jpl.nasa.gov/dsndocs/810-005>.
- [15] B. Moision, J. Wu, and S. Shambayati, "An optical communications link design tool for long-term mission planning for deep-space missions," in *2012 IEEE Aerospace Conference*, March 2012, pp. 1-12.
- [16] R. J. Barron and D. M. Boroson, "Analysis of capacity and probability of outage for free-space optical channels

with fading due to pointing and tracking error," vol. 6105, 2006, pp. 6105 - 6105 - 12. [Online]. Available: <https://doi.org/10.1117/12.638980>

- [17] A. Berk, L. Bernstein, and D. Robertson, "Modtran: A moderate resolution model for lowtran," Air Force Geophysics Laboratory, Tech. Rep. GL-TR-89-0122, 1989.

BIOGRAPHY



Hua Xie received the Ph.D. degree in electrical engineering from USC in 2004. Since then she has been with the Jet Propulsion Laboratory (JPL), California Institute of Technology (Caltech). At JPL, she has been a major contributor to development of technologies for hy-perspectral image compression, collaborative data compression for sensor networks, and region-of-interest data compression for big data in space applications. Since 2008, she has been involved in development of system engineering analysis tools for architecture study of deep space optical communications. The focus of her current work is on algorithm and software development for DSN common platform receivers.



Kar-Ming Cheung is a Principal Engineer and Technical Group Supervisor in the Communication Architectures and Research Section (332) at JPL. His group supports design and specification of future deep-space and near-Earth communication systems and architectures. Kar-Ming Cheung received NASA's Exceptional Service Medal for his work on Galileo's onboard image compression scheme. Since 1987, he has been with JPL where he is involved in research, development, production, operation, and management of advanced channel coding, source coding, synchronization, image restoration, and communication Analysis schemes. He got his B.S.E.E. degree from the University of Michigan, Ann Arbor, in 1984, and his M.S. and Ph.D. degrees from California Institute of Technology in 1985 and 1987, respectively.